Proceedings of the 2016 IEEE
International Conference on Robotics and Biomimetics
Qingdao, China, December 3-7, 2016

# Dynamics Modeling and Simulation for a Gliding Robotic Dolphin

Zhengxing Wu, Xiang Yang, Chao Zhou, Jun Yuan, and Junzhi Yu

***Abstract*— This paper provides a detailed hydrodynamic analysis of the gliding motion for a gliding robotic dolphin. In order to realize both high maneuverability and long endurance, a novel gliding robotic dolphin is developed through introducing a buoyancy-driven system for the gliding motion. Concerning the particular controllable pectoral fins and horizontal fluke of the robotic dolphin which are significantly different from traditional underwater gliders, a first-principles based dynamic model of the gliding motion in the vertical plane for the robotic dolphin is established. For the sake of determining some key hydrodynamic coefficients including lift, drag and pitching moment, the Computational Fluid Dynamics (CFD) methods are adopted for the dolphin body, pectoral fins and horizontal fluke, respectively. Specially, several prismatic layers are stacked onto the surface mesh for accurate imitation. Finally, simulation results reveal the detailed gliding performance and verify an expected gliding ability of the developed gliding robotic dolphin.**

## I. Introduction

Robotic dolphins, inspired by natural dolphins in huge oceans, have attracted considerable attention in recent years [1]–[3]. Through replicating the dorsoventral oscillations of dolphins, they have great potential to obtain the similar surprised swimming skills such as high maneuverability, high propulsive speed and low noisy which are far better than normal man-made autonomous underwater vehicles. The robotic dolphin is expected to take the place of autonomous underwater vehicles to execute some special tasks in complex underwater environments.

In fact, dolphin-like swimming has been focused on for a very long time in history. The biologists have early started their studies and published various relevant research results which can provide great inspiration and reference for the robotic dolphin researches [4]–[6]. Then, as an excellent platform, robotic dolphins have been increasingly developed to explore profound mysteries of the dolphin-like swimming. Nakashima *et al.* provided two generations of robotic dolphins with two pitch joints for three-dimensional maneuverability [7]; Yu *et al.* proposed a closed-loop pitch angle control strategy to realize excellent acrobatic maneuvers such as frontflip and backflip (360° rotation in the vertical plane) [8]; later they also developed a fast-swimming robotic dolphin which can easily leap out of the water [9]; Shen *et al.* gave a fuzzy PID controller for a robotic dolphin to realize depth control [10]; Ren *et al.* provided an average propulsive speed implementation approach for a robotic dplphin [11]; Cao *et al.* proposed a heading controller based on a self-turning fuzzy strategy for a robotic dolphin to improve control accuracy and stability [12]. Though successfully implementing dolphin-like swimming and turning maneuvers, the robotic dolphin still has many issues to solve before practical applications, including high precision positioning and navigation, long endurance, underwater communication and so on.

As we know, underwater gliders have excellent capability of long endurance, because of their particular gliding motion, e.g., the updated Slocum G2 could be able to last up to nearly 360 days [13]. Many researches have been conducted for the gliding motion since it was first provided by Stommel in 1989 [14]–[16]. Considering the poor endurance of robotic dolphins, we have previously introduced gliding motion into a robotic dolphin and developed a gliding robotic dolphin, which can not only realize fast and dolphin-like swimming due to a powerful dorsoventral mechanism, but also achieve gently and durable gliding motion depending on a buoyancy-driven system [17].

The main purpose of this paper is to propose a detailed hydrodynamic analysis in the gliding motion of a gliding robotic dolphin. Based on the first principles, we established the dynamic model of the gliding motion in a vertical plane. Considering the robotic dolphin has controllable pectoral fins and flatten fluke which is different with traditional underwater gliders, we conducted their hydrodynamic analysis, respectively. Moreover, the Computational Fluid Dynamics (CFD) methods are adopted to obtain the hydrodynamic coefficients of the gliding robotic dolphin, including the dolphin body, pectoral fins and horizontal fluke. Finally, simulation results have been given to analyze the gliding performance of the robotic dolphin.

The rest of this paper is organized as follows. The overall description of the mechanical design for the gliding robotic dolphin is provided in Section II. Section III gives the detailed analysis in the gliding motion in the vertical plane. Simulations in the gliding motion are further offered in Section IV. Finally, concluding remarks are given in Section V.

## II. Mechanical Design

Fig. 1 presents the developed gliding robotic dolphin which modeled after a killer whale for a well-streamlined body shape and also an expected space utilization rate.

This work was supported in part by the National Natural Science Foundation of China under Grants 61375102, 61473295, 61273352 and 61333016, by the Beijing Natural Science Foundation under Grants 3141002, 4152054 and 4164103, and by the Early Career Development Award of SKLMCCS, and by the National Defense Science and Technology Innovation Fund of Chinese Academy of Sciences (CXJJ-16M110).

Z. Wu, X. Yang, C. Zhou, J. Yuan, and J. Yu are with the State Key Laboratory of Management and Control for Complex Systems, Institute of Automation, Chinese Academy of Sciences, Beijing 100190, China.
(e-mail: zhouchao@compsys.ia.ac.cn)

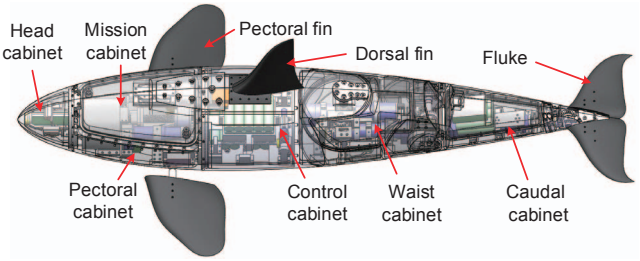


Fig. 1. Mechanical design of the gliding robotic dolphin.

TABLE I
TECHNICAL SPECIFICATION OF THE DEVELOPED GLIDING ROBOTIC DOLPHIN

| Items | Characteristics |
|---|---|
| Size ($L \times W \times H$) | $\sim 1.13 \times 0.19 \times 0.21$ m$^3$ |
| Total mass | $\sim 18.2$ kg |
| Body joints | 3 (Pitch: 2; Yaw: 1) |
| Drive mode | DC motors, Digital servomotor |
| On-board sensors | Attitude transducer, Depth sensor |
| Controller | ARM Cortex-M4 |
| Power | NCR 18650B |

Mechanically, the robotic dolphin adopts a distinctive modularity concept and is divided into six cabinets by function, including a head cabinet, a pectoral cabinet, a mission cabinet, a control cabinet, a waist cabinet and a caudal cabinet. Every cabinet contains some mechanical structures and electrical components related to their own functional requirements, such as an obstacle avoidance module in the head cabinet and a pectoral driving mechanism in the pectoral cabinet. Specially, two pitching joints respectively called waist and cauda are employed to execute symmetrical dorsoventral oscillations in a sinusoidal fashion for a fast dolphin-like swimming. Besides, a yawing joint in the waist cabinet is also employed to perform planar turning maneuvers. A pair of pectoral fins with separate degrees of freedom is designed to adjust attitude in gliding motion and also to perform multimodal locomotion including forward swimming, turning, diving and surfacing. It is worth mentioning that all the fins and fluke adopt the same airfoil, NACA0018, for a better hydrodynamic performance in a slow gliding motion. Various processing materials are adopted for the gliding robotic dolphin, such as Polyformaldehyde (POM) for most hard shells, Polymethylmethacrylate (PMMA) for the transparent shell of the head cabinet, Polypropylene (PP) for fins and fluke, aluminium alloy and titanium alloy for machinery skeletons and elements. The gliding robotic dolphin is about 1.13 m long and weighs about 18.20 kg. Table I tabulates the basic technical parameters of the robotic prototype.

To achieve a successful gliding motion, traditional underwater gliders always have two important components, a buoyancy-driven system to change the buoyancy and a moving-mass system to adjust the gliding attitude. For a gliding robotic dolphin, the latter is optional because of the controllable pectoral fins and flatten fluke. However,

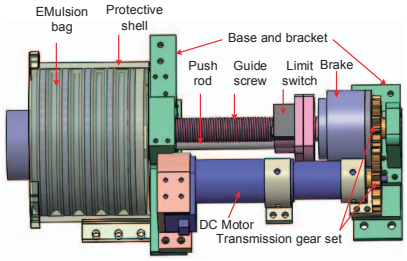


(a) The buoyancy-driven system.

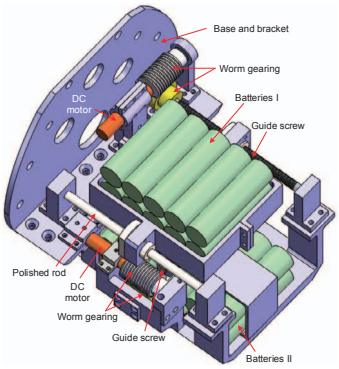


(b) The weight-adjust system.

Fig. 2. Mechanical design of the buoyancy-driven system and weight-adjust system.

the gliding robotic dolphin with a moving-mass system can obtain a better gliding attitude regulation. Given this, the robotic dolphin developed in this paper has both a buoyancy-driven system and a moving-mass system. Specially, the practical buoyancy-driven system in the pectoral cabinet changes the buoyancy through draining off and pumping the water in a emulsion bag, as shown in Fig. 2(a). With a powerful driven DC motor in buoyancy-driven system, the robotic dolphin can change the buoyancy timely and quickly. The moving-mass system employs two groups of worm gearing and guide screws to move the lithium batteries forward and backward or side to side, as shown in Fig. 2(b). So the robotic dolphin can regulate its gliding attitude in three dimensional space with ease.

## III. MOTION MODEL FOR THE GLIDING ROBOTIC DOLPHIN

In this section, we will develop a full dynamic model for the robotic dolphin gliding in water. Different from traditional gliders in previous works [18]–[20], the gliding robotic dolphin has controllable pectoral fins and flattened fluke which will bring different hydrodynamic effects in different states. Therefore, we should separately analyze the hydrodynamics of the dolphin body, pectoral fins and flattened fluke of the gliding robotic dolphin.

### A. Determination of Coordinate Systems

To clearly describe the gliding motion of the robotic dolphin, some reference frames should be defined. Fig. 3 shows two reference frames, including an inertial frame and a body reference frame. The inertial frame is described by

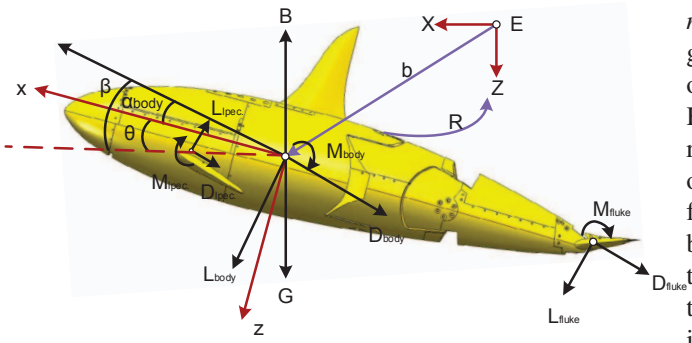


Fig. 3. Coordinate systems defined to describe the steady gliding motion.

$E_{XYZ}$, where the horizontal axes of $X$ and $Y$ are perpendicular to the gravity, and the $Z$ axis is along the positive gravity direction. The body reference frame $o_{xyz}$ is established in the center of buoyancy (CB) of the robotic dolphin, where the $x$ axis is along the longitudinal axis of the robotic dolphin from fluke to head, and the $y$ axis is located in the plane of the pectoral shafts and $z$ axis follows the right-hand rule. Define $\mathbf{R}$ as the rotation matrix from the body frame to the inertial frame coordinates. Let $\mathbf{b} = (x, y, z)^T$ denote the position of the glider, which is the vector from the origin of the inertial frame to the origin of the body frame. Let $\alpha_{body}$ and $\theta$ indicate the angle of attack and the pitch angle of the dolphin body in vertical plane. $B$ and $G$ separately denotes the buoyancy and gravity of the robotic dolphin. $L_i, D_i, M_i$ ($i =$ body, lpec, rpec and fluke) represents the hydrodynamic lift, drag and moment on the body, left pectoral fin, right pectoral fin and the flatten fluke, respectively.

The total mass of the gliding robotic dolphin $m_t$ consists of three terms: $m_t$=$m_h + m_w + m_b$. $m_h$ is a fixed mass including the mass of body hull, pectoral fins and horizontal fluke that is uniformly distributed throughout the body of the robotic dolphin. $m_w$ is also a fixed point mass which may be offset $\mathbf{r_w}$ from the CB. $m_b$ is the variable ballast point mass, which may also be offset $\mathbf{r_b}$ from the CB. The moving internal point mass is $m_s$, which is indeed the mass of lithium batteries. So we can get the total mass of the gliding robotic dolphin is then $m_v = m_h + m_w + m_b + m_s = m_t + m_s$. In particular, we design the pectoral shafts passing through the center of the mass (CM) of the pectoral fins, and also the fluke shaft passes through the CM of the flatten fluke. So we can ignore the variation of the CM while the pectoral fins and fluke turning. Besides, we define the mass of the displaced fluid as $m$, So the net buoyancy $m_0$ can be defined by $m_0 = m_v - m$. Thus the robotic dolphin is negatively (positively) buoyant if $m_0$ is positive (negative).

### B. Motion Model in Vertical Plane

Considering the major design elements of traditional underwater gliders, such as buoyancy control, wings and external control surfaces, internal mass actuators and so on, Grave *et al.* firstly developed a general, first-principles based model of the dynamic of an underwater glider [18], [19]. Then, through eliminating the offset static mass by setting $m_w = 0$, and fixing the ballast mass at the centroid of the glider body by $r_b = 0$, Grave *et al.* provided the equations of motion for the underwater gliders in the vertical plane. Here we adopt the similar analysis [18]. For the gliding robotic dolphin, the main differences includes two aspects: one is that we should separately analyze the hydrodynamic forces on the dolphin body, pectoral fins and flattened fluke because they can be controlled for a better gliding motion, the other is that we should consider the pitching torque from the buoyancy system because it is fixed in the head but not in the CM of gliding robotic dolphin. Based on the previous work from Grave, it is easy to get the vertical plane gliding motion equations for the gliding robotic dolphin as follows:

$$\dot{x} = v_x \cos\theta + v_z \sin\theta \quad (1)$$

$$\dot{z} = -v_x \sin\theta + v_z \cos\theta \quad (2)$$

$$\dot{\theta} = \Omega_y \quad (3)$$

$$\begin{aligned}\dot{\Omega}_y = \frac{1}{J_y}&((m_z - m_x)v_x v_z - (P_{b_x} r_{b_x} + P_{b_z} r_{b_z})\Omega_y \\ &-(P_{s_x} r_{s_x} + P_{s_z} r_{s_z})\Omega_y - m_b g(r_{b_x}\cos\theta + r_{b_z}\sin\theta) \\ &-m_s g(r_{s_x}\cos\theta + r_{s_z}\sin\theta) + M_{DL_{Total}} \\ &-(u_{b_x} r_{b_z} - r_{b_x} u_{b_z}) - (u_{s_x} r_{s_z} - r_{s_x} u_{s_z}))\end{aligned} \quad (4)$$

$$\begin{aligned}\dot{v}_x = \frac{1}{m_x}&(-[m_z v_z + P_{b_z} + P_{s_z}]\Omega_y - m_0 g\sin\theta \\ &+L_{Total_x} + D_{Total_x} - u_{b_x} - u_{s_x})\end{aligned} \quad (5)$$

$$\begin{aligned}\dot{v}_z = \frac{1}{m_z}&([m_x v_x + P_{b_x} + P_{s_x}]\Omega_y + m_0 g\cos\theta \\ &+L_{Total_z} + D_{Total_z} - u_{b_z} - u_{s_z})\end{aligned} \quad (6)$$

$$\dot{r}_{b_x} = \frac{1}{m_b} P_{b_x} - v_x - \Omega_y r_{b_z} \quad (7)$$

$$\dot{r}_{b_z} = \frac{1}{m_b} P_{b_z} - v_z + \Omega_y r_{b_x} \quad (8)$$

$$\dot{r}_{s_x} = \frac{1}{m_s} P_{s_x} - v_x - \Omega_y r_{s_z} \quad (9)$$

$$\dot{r}_{s_z} = \frac{1}{m_s} P_{s_z} - v_z + \Omega_y r_{s_x} \quad (10)$$

$$\dot{P}_{b_x} = u_{b_x} \quad (11)$$

$$\dot{P}_{b_z} = u_{b_z} \quad (12)$$

$$\dot{P}_{s_x} = u_{s_x} \quad (13)$$

$$\dot{P}_{s_z} = u_{s_z} \quad (14)$$

$$\dot{m}_b = \rho S_b v_b \quad (15)$$

where, $v_i$ ($i = x,\ z$) and $\Omega_y$ is separately the translational velocity relative to the inertial frame and angular velocity, both expressed in the body frame. $m_i (i = x,\ z)$ is the sum of body and added mass in $i$th axis. $J_y$ is the total inertia including added inertia and the robotic dolphin in $y$ axis. $P_{b_i}$ and $P_{s_i}$ denote the ballast mass and moving internal mass momenta in the body frame. $u_{b_i}$ and $u_{s_i}$ are the control force in the ballast mass and moving internal mass, respectively. $L_{Total}, D_{Total}$ and $M_{DL_{Total}}$ denotes separately the total hydrodynamic lift, drag and the viscous moment on the

gliding robotic dolphin, and they can be expressed as follows:

$$L_{Total_x} = (L_{body} + L_{lpec} + L_{rpec} + L_{fluke}) \sin \alpha_{body}$$
$$L_{Total_z} = -(L_{body} + L_{lpec} + L_{rpec} + L_{fluke}) \cos \alpha_{body}$$

$$D_{Total_x} = -(D_{body} + D_{lpec} + D_{rpec} + D_{fluke}) \cos \alpha_{body}$$
$$D_{Total_z} = -(D_{body} + D_{lpec} + D_{rpec} + D_{fluke}) \sin \alpha_{body}$$

As for the buoyancy-driven system, we only consider its pitching torques for the gliding robotic dolphin, and ignore the variation of the CM caused by the moving of emulsion bag. Therefore, we have $\dot{r}_{bx} = 0$ and $\dot{r}_{bz} = 0$. According to these expressing equations of $\dot{r}_{bx}$ and $\dot{r}_{bz}$ above, we can easily obtain these following equations.

$$P_{bx} = m_b(v_x + \Omega_y r_{bz}) \quad (16)$$
$$P_{bz} = m_b(v_z - \Omega_y r_{bx}) \quad (17)$$
$$\dot{P}_{bx} = \dot{m}_b(v_x + \Omega_y r_{bz}) + m_b(\dot{v}_x + \dot{\Omega}_y r_{bz} + \Omega_y \dot{r}_{bz}) \quad (18)$$
$$\dot{P}_{bz} = \dot{m}_b(v_z - \Omega_y r_{bx}) + m_b(\dot{v}_z - \dot{\Omega}_y r_{bx} - \Omega_y \dot{r}_{bx}) \quad (19)$$

According to these expressing equations of $\dot{r}_{sx}$ and $\dot{r}_{sz}$ above, we can easily obtain the momentum of the moving internal masses and even their differential form as follows:

$$P_{sx} = m_s(v_x + \Omega_y r_{sz} + \dot{r}_{sx}) \quad (20)$$
$$P_{sz} = m_s(v_z - \Omega_y r_{sx} + \dot{r}_{sz}) \quad (21)$$
$$\dot{P}_{sx} = m_s(\dot{v}_x + \dot{\Omega}_y r_{sz} + \Omega_y \dot{r}_{sz} + \ddot{r}_{sx}) \quad (22)$$
$$\dot{P}_{sz} = m_s(\dot{v}_z - \dot{\Omega}_y r_{sx} - \Omega_y \dot{r}_{sx} + \ddot{r}_{sz}) \quad (23)$$

Based on these above equations (17)–(24), we can obtain the new motion equations to replace (4)–(6).

$$(m_x + m_b + m_s)\dot{v}_x = Q_1 - \dot{m}_b(v_x + \Omega_y r_{bz}) - \dot{\Omega}_y(m_b r_{bz} + m_s r_{sz}) - m_s \ddot{r}_{sx} \quad (24)$$
$$(m_z + m_b + m_s)\dot{v}_z = Q_2 - \dot{m}_b(v_z - \Omega_y r_{bx}) + \dot{\Omega}_y(m_b r_{bx} + m_s r_{sx}) - m_s \ddot{r}_{sz} \quad (25)$$

$$(J_y + J_b' + J_s')\dot{\Omega}_y = Q_3 - \dot{m}_b((v_x + \Omega_y r_{bz}) r_{bz} - (v_z - \Omega_y r_{bx}) r_{bx}) - (m_b r_{bz} + m_s r_{sz})\dot{v}_x + (m_b r_{bx} + m_s r_{sx})\dot{v}_z - m_s r_{sz} \ddot{r}_{sx} - m_s r_{sx} \ddot{r}_{sz} \quad (26)$$

Here, we have

$$Q_1 = -\Omega_y[m_z v_z + m_b(v_z - \Omega_y r_{bx}) + m_s(v_z - \Omega_y r_s x + \dot{r}_{sz}) + m_b \dot{r}_{sz}] - m_0 g \sin\theta + L_{Total_x} + D_{Total_x}$$
$$Q_2 = \Omega_y[m_x v_x + m_b(v_x + \Omega_y r_{bz}) + m_s(v_x + \Omega_y r_{sz} + \dot{r}_{sz}) + m_s \dot{r}_{sx}] + m_0 g \cos\theta + L_{Total_z} + D_{Total_x}$$
$$Q_3 = (m_z - m_x)v_x v_z - \Omega_y[m_b(r_{bx} v_x + r_{bz} v_z) + m_s r_{sx} v_x + m_s r_{sz} v_z + 2m_s r_{sz} \dot{r}_{sz} + 2m_s r_{sx} \dot{r}_{sx}] - m_b g(r_{bx} \cos\theta + r_{bz} \sin\theta) - m_s g(r_{sx} \cos\theta + r_{sz} \sin\theta) + M_{DL_{Total}}$$

For now, we get the whole hydrodynamic model of the gliding motion of the robotic dolphin.

### C. Hydrodynamic Analysis

In the following part, we will present the form of the hydrodynamic terms in the glider dynamic equations, including hydrodynamic forces and moments which are from both viscous and inviscous effects. Since modelling the glider in the vertical, longitudinal plane, these hydrodynamic forces and moments can be modelled as follows [19].

$$L_i = \frac{1}{2}\rho C_{L_i}(\alpha_i) S_i v^2 \quad (27)$$
$$D_i = \frac{1}{2}\rho C_{D_i}(\alpha_i) S_i v^2 \quad (28)$$
$$M_i = \frac{1}{2}\rho C_{M_i}(\alpha_i) S_i v^2 \quad (29)$$

where $i =$ body, lpec, repc and fluke denotes the related variable about the dolphin body, left pectoral fin, right pectoral fin and flattened fluke. $\rho$ indicates the fluid density. $v$ denotes the relative velocity of the robotic dolphin respect to the fluid. $\alpha_i$ indicates the angle of attack of the robotic dolphin, and $\alpha_i$ ($i =$ lpec, repc and fluke) can be obtained through $\alpha_{\text{body}}$ and turn angles of pectoral fins and fluke. $C_{L_i}, C_{D_i}, C_{M_i}$ are the standard aerodynamic lift, drag and moment coefficients by cross sectional area for dolphin body, pectoral fins and fluke. $S_i$ denotes the maximum cross sectional area.

Here, CFD methods are employed to obtain the hydrodynamic force coefficients including $C_{L_i}, C_{D_i}, C_{M_i}$ of the gliding robotic dolphin. Because the pectoral fins and flattened fluke can be controlled, we need separately compute the hydrodynamic coefficients about the dolphin body, pectoral fins and flattened fluke. Take the body of the gliding robotic dolphin for example. In the pre-processing meshing work, an unstructured tetrahedron mesh is formed to describe the flow domain for great adaptability and high quality, as shown in

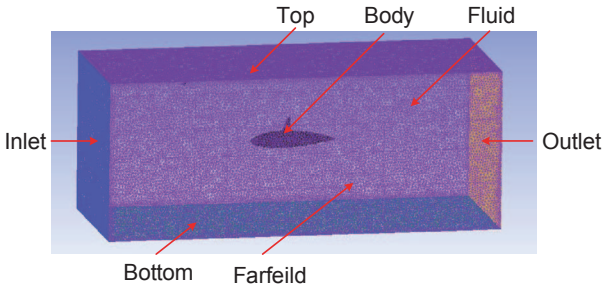


(a) Boundary conditions for the gliding robotic dolphin.

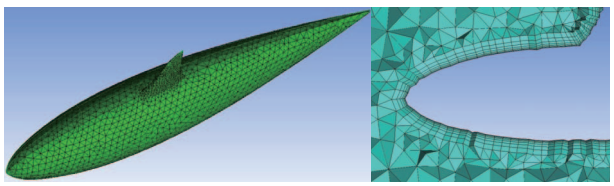

(b) Surface mesh of the body (left) and Cut-plan of volume mesh around of the cylindrical body (right).

Fig. 4. Boundary conditions and unstructured tetrahedron mesh for the gliding robotic dolphin.

Fig. 4(a). Meanwhile, seven prismatic layers are stacked onto the surface mesh for accurate simulation results, as shown in Fig. 4(b). The whole computational domain of the dolphin body is surrounded by the following boundaries:

1) Inlet boundary: 2.5 body lengths from the nose and set as velocity-inlet with $v = 0.3$ m/s;
2) Outlet boundary: 2.5 body lengths from the fluke and set as outflow;
3) Top and Bottom boundaries: set as velocity-inlet with $v = 0.3$ m/s in order to avoid reflected effect;
4) Farfeild boundary: set as no-flip walls;
5) Surface boundary: set as no-slip moving walls.

The CFD computational domain for the pectoral fins and flattened fluke adopt the similar boundary conditions. Moreover, we assume the fluid is incompressible and steady, and k–$\omega$ SST (Shear-Stress-Transport) turbulence model with low-Re corrections is employed in Fluent simulation.

When gliding in a vertical plane, the hydrodynamic coefficients could be simplified as a function about the angle of attack, e.g., quadratic polynomial for a drag coefficient and monomial for lift coefficient according to previous results [19]. As for the dolphin body, we adopt the quartic polynomial to fit the curves of the hydrodynamic coefficients of the dolphin body for more accuracy results and the quadratic polynomial and monomial for the pectoral fins and flattened fluke. The hydrodynamic coefficients about the dolphin body, pectoral fins and flattened fluke are fitted as follows:

$$\begin{cases} C_{d_{\text{body}}}(\alpha) &= 4.749\alpha^4 - 0.111\alpha^3 \\ & \quad +0.556\alpha^2 - 0.007\alpha + 0.148 \\ C_{l_{\text{body}}}(\alpha) &= -1.833\alpha^4 + 4.997\alpha^3 \\ & \quad -0.072\alpha^2 + 0.485\alpha - 0.006 \\ C_{m_{\text{body}}}(\alpha) &= 0.220\alpha^4 + 1.407\alpha^3 \\ & \quad -0.050\alpha^2 - 0.097\alpha + 0.005 \end{cases} \tag{30}$$

$$\begin{cases} C_{d_{\text{pec}}}(\alpha) &= 1.555\alpha^2 - 0.003\alpha + 0.034 \\ C_{l_{\text{pec}}}(\alpha) &= 1.725\alpha \\ C_{m_{\text{pec}}}(\alpha) &= -0.314\alpha \end{cases} \tag{31}$$

$$\begin{cases} C_{d_{\text{fluke}}}(\alpha) &= 1.920\alpha^2 - 0.003\alpha + 0.069 \\ C_{l_{\text{fluke}}}(\alpha) &= 2.260\alpha \\ C_{m_{\text{fluke}}}(\alpha) &= 1.424\alpha \end{cases} \tag{32}$$

## IV. Simulation and Results

The simulations are executed to explore the gliding performance of the robotic dolphin in this section. At first, the robotic dolphin realizes the gliding motion depending on both controllable fins and the internal moving mass. Specially, it will perform three actions for gliding upwards or downwards, including pumping or draining off some water through buoyancy-driven system, turning the pectoral fins in negative or positive direction, and moving the lithium batteries forward or backward. For simplicity, we assume that the internal moving mass only has one degree of freedom in $x$ axis. The model parameters adopted in simulations are given as follows: $m_v = 18.20$, $m_b = 0.18$, $m_s = 0.8$, $m_x = 12.24$, $m_z = 45.70$, $J_y = 0.46$, $r_{b_x} = 0.25$, $r_{b_z} = 0$, $r_{s_x} = 0.025$, $r_{s_z} = 0$.

Fig. 5 and Fig. 6 show the gliding path of the robotic dolphin. We can see that, under the action of these three control inputs, the robotic dolphin successfully realizes the sawtooth motions. In these simulations, the robotic dolphin glides following a 200-second cycle. In the first 100 seconds, the robotic dolphin keeps a downwards gliding motion to about 13.18 meters depth, and then begins to glide upwards in the following 100 seconds. According to the Fig. 5, we can see that the robotic dolphin actually glides in a almost straight line in the horizontal plane, although a particular sawtooth motion is executed in the vertical plane, as shown in Fig. 6.

Fig. 7 and Fig. 8 illustrate the gliding velocity in $x$ axis and $z$ axis, respectively. As for the underwater gliders, the gliding velocity is decided by the variable buoyancy mass and hydrodynamic coefficients, including hydrodynamic lift and drag. In simulations, we can see that the robotic dolphin can reach a maximum steady gliding velocity with about 0.21 m/s in $x$ axis, and about $-0.08$ m/s in $z$ axis.

## V. Conclusions and Future Work

In this paper we have developed a gliding motion model for a gliding robotic dolphin which is to obtain both high maneuverability and long endurance. Concerning the controllable pectoral fins and horizontal fluke and even the pitching torques from the buoyancy-driven system in the head, a dynamic model based on first-principles of the robotic dolphin gliding in water is established. In order to obtain the key hydrodynamic coefficients including lift, drag and moment coefficients, CFD methods are adopted and applied for the simulation of dolphin body, pectoral fins and

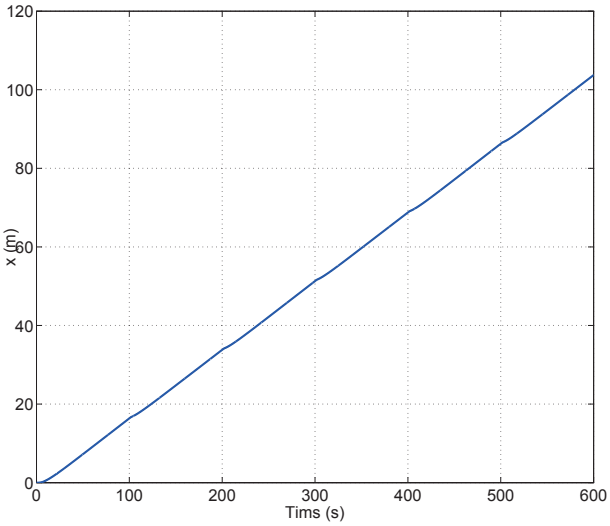


Fig. 5. Gliding path in the horizontal plane.

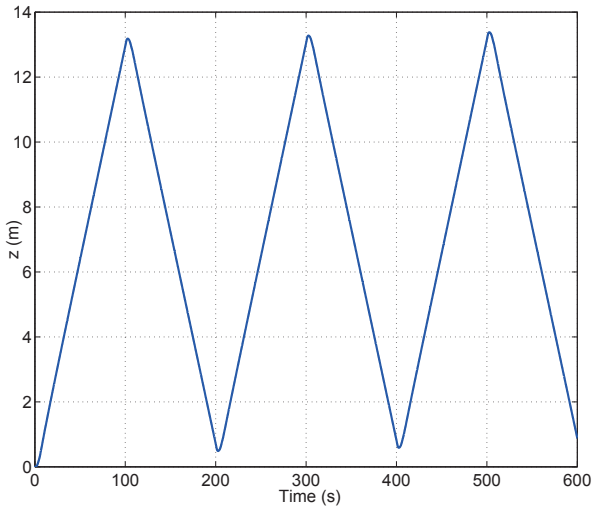


Fig. 6. Gliding path in the vertical plane.

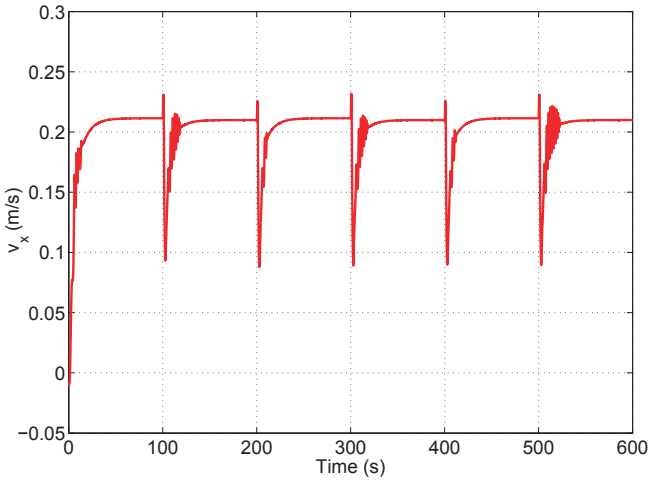


Fig. 7. Gliding velocity in the horizontal plane.

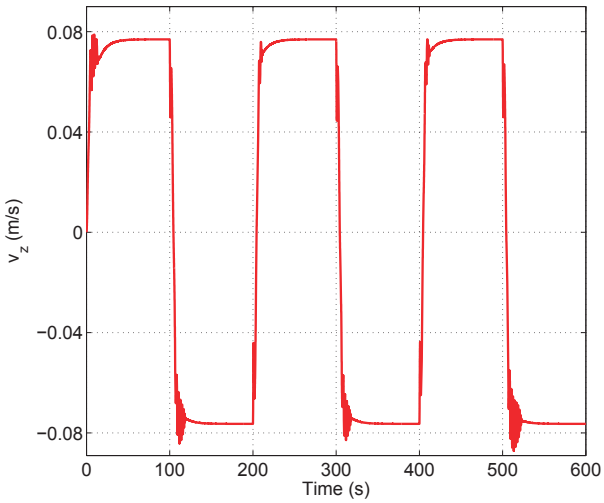


Fig. 8. Gliding velocity in the vertical plane.

horizontal fluke, respectively. Simulations in gliding motions verify the great gliding ability of the gliding robotic dolphin.

The ongoing and future work will focus on the closed-loop gliding control for the robotic dolphin based on the pectoral fins and horizontal fluke, since the robotic dolphin can effectively employ these fins to regulate the gliding attitude.

## REFERENCES


[1] G. Dogangil, E. Ozcicek, and A. Kuzucu, "Modeling, simulation, and development of a robotic dolphin prototype," in *Proc. IEEE Int. Conf. Mechatron. Autom.*, Canada, Jul. 2005, pp. 952–957.

[2] Y. Park, K. Cho, "Design and manufacturing a bio-inspired variable stiffness mechanism in a robotic dolpin," in *Intelligent Robotics and Applications*, vol. 8103, pp. 302–309, 2013.

[3] J. Yu, and C. Wei, "Towards development of a slider-crank centered self-propelled dolphin robot," in *Advanced Robotics*, vol. 27, no. 12, pp. 971–977, 2013.

[4] F. E. Fish and J. J. Rohr, "Review of dolphin hydrodynamics and swimming performance," U.S. Navy, San Diego, CA, Tech. Rep. 1801, Aug. 1999.

[5] M. Nagai, *Thinking Fluid Dynamics with Dolphins.* Tokyo, Japan: Ohmsha, 2002.

[6] F. E. Fish, "Drag reduction by dolphins: Myths and reality as applied to engineered designs," *Bioinsp. Biomim.*, vol. 1, pp. R17–R25, 2006.

[7] M. Nakashima, T. Tsubaki, and K. Ono, "Three-dimensional movement in water of the dolphin robot-Control between two positions by roll and pitch combination," *J. Robot. Mechatron.*, vol. 18, no. 3, pp. 347–355, 2006.

[8] J. Yu, Z. Su, M. Wang, M. Tan, and J. Zhang, "Control of yaw and pitch maneuvers of a multilink dolphin robot," *IEEE Trans. Robot.,* vol. 28, no. 2, pp. 318–329, 2012.

[9] J. Yu, Z. Su, Z. Wu, and M. Tan, "An integrative control method for bio-inspired dolphin leaping: design and experiments," *IEEE Transactions on Industrial Electronics*, vol. 63, no. 5, pp. 3108–3116, 2016.

[10] S. Shen, Z. Cao, C. Zhou, D. Xu, and N. Gu, "Depth control for robotic dolphin based on fuzzy PID control," *International Society of Offshore and Polar Engineers,* vol. 23, no. 3, 2013.

[11] G. Ren, Y. Dai, Z. Cao, and F. Shen, "Research on the implementation of average speed for a bionic robotic dolphin," *robotics and Autonomous Systems,* vol. 74, pp. 184–194, 2015.

[12] Z. Cao, F. Shen, C. Zhou, N. Gu, S. Nahavandi, and D. Xu, "Heading control for a robotic dolphin based on a self-tuning fuzzy strategy," *International Journal of Advanced Robotic Systems,* vol. 13, no. 28, pp.1–8, 2016.

[13] TWR, http://www.webbresearch.com/slocumglider.aspx

[14] H. Stommel, "The slocum mission," *Oceanography*, vol. 2, no. 1, pp. 22–25, 1989.

[15] S. Zhang, J. Yu, A. Zhang, and F. Zhang, "Spiraling motion of underwater gliders: modeling, analysis, and experimental results," *Ocean Engineering*, vol. 60, pp. 1–13, 2013.

[16] K. Isa, M. R. Arshad, and S. Ishak, "A hydrid-driven underwater glider model, hydrodynamics estimation, and an analysis of the motion control," *Ocean Engineering*, vol. 81, pp. 111–129, 2014.

[17] Z. Wu, J. Yu, J. Yuan, M. Tan and J. Zhang, "Mechatronic design and implementation of a novel gliding robotic dolphin," in *Proc. IEEE IEEE Int. Conf. Robot. Biomim.*, Zhuhai, China, Dec. 2015, pp.267–272.

[18] J. G. Graver, R. Bachmayer, N. E. Leonard, and D. M. Fratantoni, "Underwater glider model parameter identification," in *Proc. 13th Int. Symp. on Unmanned Untethered Submersible Technology*, August 2003, pp. 1–12.

[19] J. G. Graver, "Underwater gliders: Dynamics, control and design," [Ph.D. dissertation], Princeton University, USA, May 2005.

[20] A. A. H. Nur, R. A. Mohd, and M. Rosmiwati, "Underwater glider modelling and analysis for net buoyancy, depth and pitch angle control," in *Ocean Engineering*, vol. 38, no. 16, pp. 1782–1791, 2011.